Molecular dynamics simulation of the structure of yttria Y_2O_3 phases using pairwise interactions

A. B. Belonoshko,[1] G. Gutierrez,[2,3] R. Ahuja,[2] and B. Johansson[1,2]
[1]*Applied Materials Physics, Department of Materials Science and Engineering, The Royal Institute of Technology, SE-100 44 Stockholm, Sweden*
[2]*Condensed Matter Theory Group, Department of Physics, Uppsala University, Box 530, S-751 21, Uppsala, Sweden*
[3]*Departamento de Fisica, Universidad de Santiago, Casilla 306, Santiago 2, Chile*
(Received 2 September 2000; revised manuscript received 26 February 2001; published 16 October 2001)

We have studied the structure of yttria (Y_2O_3) by means of *ab initio* and molecular dynamics methods. The suggested simple model for the interatomic interaction is shown to produce reasonable results at moderate pressures for a wide range of temperatures. The calculated x-ray structure factor is in good agreement with experimental data obtained by the x-ray levitation technique at the temperature of 2526 K. The quality of the agreement decreases with increasing temperature. We demonstrate that it is not necessary to assume nonstoichiometry of liquid yttria, as was done in a recent publication, to obtain agreement with experiment. The structure of liquid yttria can be considered as a mixture of 4- and 6-coordinated Y atoms. We also show the possibility of a ''light'' amorphous yttria phase, which possibly can be obtained by quenching from a vapor instead of ''conventional'' amorphous yttria quenched from a liquid.

DOI: 10.1103/PhysRevB.64.184103 PACS number(s): 61.20.−p, 61.25.−f, 71.15.Nc

I. INTRODUCTION

Yttria (Y_2O_3) is an end-member component of the Al_2O_3-Y_2O_3 system. Stoichometric compounds in this system, such as perovskite (YAP) and garnet (YAG) are important technological materials.[1] On the other hand, a few years ago density-driven liquid-liquid phase separation in this system was observed.[2] Of course, it is challenging and of fundamental interest to investigate this phenomenon on an atomistic scale. Naturally, before embarking on this study, we have to be convinced that our tools are adequate for studies of simpler systems, namely, yttria and alumina (Al_2O_3). Alumina was studied and the results are in good agreement with experimental data.[3–6] Recently, valuable experimental data for the structure of liquid and undercooled yttria was obtained by a containerless technique.[7,8] However, the interpretation of this data was questioned.[9] The objective of the present study is threefold: first, to develop and test our model of yttria by comparison with experimental data; second, to provide a detailed explanation of noncrystalline yttria structure on the atomic scale; and third, to see if it is indeed necessary to assume[9] nonstoichiometric composition of liquid yttria to obtain good agreement with experiment.

The paper is organized as follows. First, the procedure for developing a model for yttria is explained. Second, some technical details of our MD simulations are provided. Third, the results concerning verification of our model and comparison between the calculated and experimental structures are given. We also show that there is a possibility of formation of a less dense amorphous phase which can be quenched from yttria vapor in MD simulation. Fourth, we discuss the results of our simulations and compare with previous results.[9]

II. INTERATOMIC POTENTIALS

In a recent study[9] of yttria the pair interaction potential of a Pauling type was used. This potential consists of two terms, namely, the Coulomb interaction and a power function as a repulsive term. Unfortunately, this interaction model[9] does not reproduce the melting temperature of yttria.[7,8]

Therefore, we felt that we could not rely on the same potential and decided to develop another one. We wanted to obtain a potential which would have as few parameters as possible, yet it should reproduce properties of the substance with a reasonable precision. For ionic materials interatomic potentials in the form of a Buckingham potential[10] is a rather traditional model which has been shown to perform sufficiently well[11–14] and, therefore, widely used for modeling of various oxides. The advantages and shortcomings of these kind of models are well known.[15] Since with increasing ionicity the van der Waals term becomes less important,[16] we assumed the interaction model to be of the following form:

$$V(r_{ij}) = \frac{Z_i Z_j e^2}{r_{ij}} + A_{ij}\exp(-B_{ij} r_{ij}), \tag{1}$$

where the individual terms represent the Coulomb and repulsion energy, respectively. Here r_{ij} is the interatomic distance between atoms i and j, Z_i is an effective charge of the ith atom, e the electron charge, and A_{ij} and B_{ij} are parameters for the repulsive interactions.

These parameters were fitted using the computer code GULP (Ref. 17) to reproduce the structure, bulk modulus (K_T), and the C_{11} and C_{12} elastic constants of yttria in the α-Y_2O_3 phase at zero pressure and zero temperature. The data for the fit was obtained as follows.

The structural form of Y_2O_3 stable up to near its melting temperature is cubic (space group $Ia3$, Mn_2O_3 bixbyite type), known as α-Y_2O_3 or C-Y_2O_3. The crystal structure was studied by x-ray diffraction[18,19] and by neutron diffraction.[20,21] This structure was chosen as an input for the fit in the lattice dynamics program GULP. The lattice constant, bulk modulus (K_T) and the C_{11} and C_{12} elastic constants were calculated using the full-potential linear muffin-

TABLE I. Parameters of the potential [Eq. (1) ($Z_Y=1.8, Z_O=-1.2$)] for Y_2O_3.

Atom-Atom	A (kJ mol)	B ($Å^{-1}$)
Y-Y	239 350.4	4.3048
Y-O	143 417.5	5.7928
O-O	450 833.3	5.3195

tin-orbital (FPLMTO) method[22] assuming the same structure. Using the FPLMTO method we also calculated energy (E)-volume(V) curve for the same (α-Y_2O_3) structure. This curve was used to obtain the P-V equation of state at zero temperature. The FPLMTO calculations were based on the local-density approximation and we used the Hedin-Lundqvist[23] parametrization for the exchange and correlation potential. Basis functions, electron densities, and potentials were calculated without any geometrical approximation.[22] These quantities were expanded in combinations of spherical harmonic functions (with a cutoff $l_{\max}=6$) inside nonoverlapping spheres surrounding the atomic sites (muffin-tin spheres) and in a Fourier series in the interstitial region. The muffin-tin sphere occupied approximately 62% of the unit cell. The radial basis functions within the muffin-tin spheres are linear combinations of radial wave functions and their energy derivatives, computed at energies appropriate to their site, principal as well as orbital atomic quantum numbers, whereas outside the spheres the basis functions are combinations of Neuman or Hankel functions.[24,25] In the calculations reported here, we made use of pseudocore $4p$ states for Y and valence band $5s$, $5p$, $4d$, and $4f$ basis functions for Y and valence band $2s$, $2p$, and $3d$ basis functions for O with corresponding two sets of energy parameters, one appropriate for the semicore $4p$ states, and the other appropriate for the valence states. The resulting basis formed a single, fully hybridizing basis set. For sampling the irreducible wedge of the Brillouin zone we used the special k-point method.[26] In order to speed up the convergence we have associated each calculated eigenvalue with a Gaussian broadening of width 20 mRy.

When using lattice dynamics for calculating the parameters of the potential [Eq. (1)], we used a so-called relaxed fitting,[17] such that atoms were allowed to change their positions in order to result in zero forces acting on them. Since in our fit we used a unit cell containing 32 Y atoms and 48 O atoms, the total number of observables is equal to 249, while the number of fitted parameters equals 8. Still, we have obtained a very good description of the fitted data. Three sets of effective charges were probed (with the effective charge on the Y atom equal to -2.1, -1.8, and -1.5e, respectively). The best fit was obtained with the parameters listed in Table I. Some results of the fit and the FPLMTO data, which was used for the fit, are listed in Table II along with the experimental data.[27]

TABLE II. Some experimental and calculated properties of yttria.

Property	Expt. (Ref. 27)	*Ab initio* (FPLMTO)[a]	Fitted
Unit cell (Å)	10.6	10.5	10.598
Bulk modulus (GPa)	156.0	154.0	154.6
C_{11}	224.0	247.0	235.0
C_{12}	90.0	107.0	114.4

[a]R. Ahuja (unpublished).

III. MOLECULAR DYNAMIC SIMULATIONS

A. Technical details

A description of the molecular dynamic method can be found elsewhere.[28] In short, the molecular dynamic method consists in solving numerically equations of atomic motion, assuming initial coordinates and velocities of atoms and a model of interaction between them. Normally, as is also the case in our MD calculations, periodic boundary conditions (PBC) are applied. PBC means that if a particle leaves a computational cell on one side of the cell, then an identical particle enters the cell from the opposite side. Most of the simulations were performed using the package MOLDY.[29] Simulations in the NTP (constant N: number of particles; T: temperature; and P: pressure) ensemble[30] were performed. The results of MD simulations in the NTP ensemble with the chosen model of the interatomic interaction depend on, apart from the initial arrangement of atoms, the number of time steps ($n_{\text{time steps}}$), size of time step (Δt), number of atoms (N), cutoff (r_{cutoff}) of the interatomic potential, specified time constants for temperature (τ_T), and pressure (τ_P) fluctuations. Therefore, the influence of these parameters was carefully studied by carrying out test runs at various T and P. It was found that correct results can normally be obtained with $n_{\text{time steps}}=20\,000$, $\Delta t=0.002$ psec, $r_{\text{cutoff}}=8$ Å, $\tau_T=0.2$ psec, and $\tau_P=0.5$ psec. Still, whenever we suspected that the results might have been affected by the choice of the above parameters we varied them to verify that the final results are correct. For example, when modeling amorphous phases (see below) at low temperatures, we performed very long runs with $n_{\text{time steps}}=200\,000$. The number of particles N was 2160 atoms, which correspond to a $3\times3\times3$ configuration of the unit cell containing 80 atoms. Some of the results were checked using $4\times4\times4$ configuration with N equal to 5120 atoms. The long-range Coulomb energy was calculated using the Ewald method[31] with a precision of 10^{-5}. The assumption of a mean-field distribution of the density was applied for the calculations of the energy and forces at $r>r_{\text{cutoff}}=8$ Å. The convergence of results was checked by calculating intermediate averages.[28]

B. Verification of the interaction model

In order to verify a reliable performance of the model at pressures (P) and temperatures (T) different from the ambient (0 bar and 298 K), we performed a series of MD simulations. The initial configuration of the Y and O atoms was the crystal lattice possessing $Ia3$ symmetry (α-Y_2O_3). The Y atoms occupies two nonequivalent positions, one in the center of a distorted cube, with only six of the eight cube corners occupied by O atoms. The other Y position is in the center of the edge-adjacent cube with differently arranged O

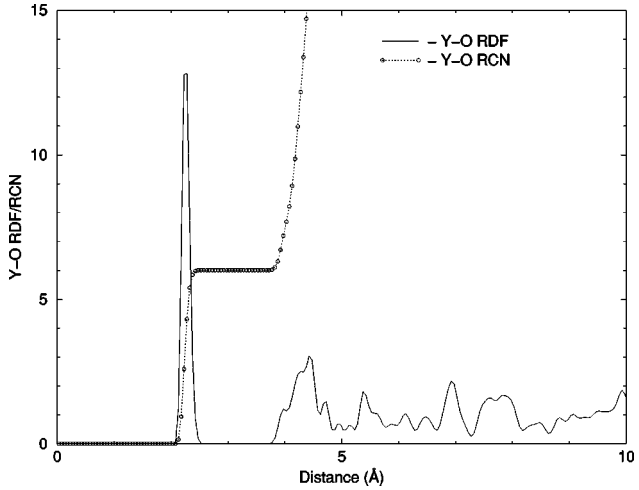

FIG. 1. The Y-O radial distribution function (RDF) of solid yttria (α-Y_2O_3) simulated by molecular dynamics (MD) method at the temperature of 300 K and pressure 1 bar. The Y-O running coordination number (RCN, average number of O atoms around Y atom as a function of distance from Y atom) is also shown. There is a step at the Y-O RCN curve which confirms that the first coordination shell of Y atom consists of 6 O atoms.

atoms. While the first type of position for Y is symmetrically surrounded by 6 O atoms, the second position is also 6 coordinated, with 3 atoms somewhat closer and 3 O atoms somewhat further away compared to the first position for Y. Nevertheless, even smaller temperature induced perturbations of the yttria structure lead to a strong first peak in the radial distribution function (RDF) of O atoms around the Y atom. The second peak of the Y-O RDF is separated from the first one by a considerable distance (Fig. 1).

Pressure-volume (PV) relationship, calculated at the temperature (T) of 300 K is shown in Fig. 2 compared with FPLMTO (0 K isotherm) curve. Note that the pressure dependence of α-Y_2O_3 volume calculated with the FPLMTO method was not used to calculate the parameters of the potential [Eq. (1)]. Since the fitted bulk modulus (Table II) compares well with the FPLMTO bulk modulus, the isotherms are close to each other up to pressures of about 10 GPa. However, at higher pressure the isotherms are rather different. Since we are interested in properties of yttria at elevated temperatures at normal pressure, which corresponds to larger volumes than at ambient T and P, the agreement is sufficiently good in the region of interest. On the other hand, we have to conclude that the developed interatomic potential is not suitable for modeling of yttria at very high pressures.

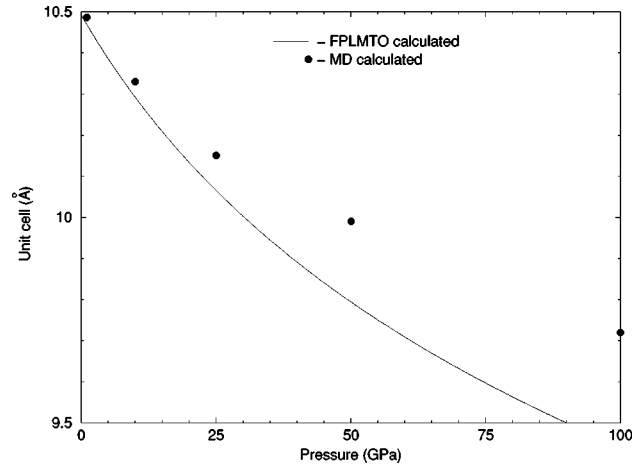

FIG. 2. The FPLMTO (0 K) and MD (300 K) calculated isotherms of solid yttria (α-Y_2O_3). The volume is given in terms of the size of the cubic unit cell containing 80 atoms (i.e., 16 formula units of yttria).

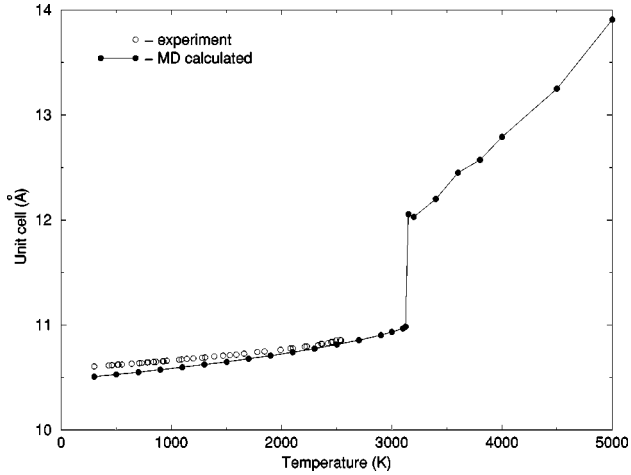

FIG. 3. The MD calculated volume of yttria at the pressure of 1 bar as a function of temperature compared with experimental data (Ref. 32) for the α-Y_2O_3. The MD calculated points are connected by dashed line for convenience. The sudden jump at a temperature of about 3150 K is an indication of thermal instability and a transition into a liquid state. The volume is given in terms of the size of the cubic unit cell containing 80 atoms (i.e., 16 formula units of yttria).

MD calculated volumes at P=1 bar and at T from 300 K up to 5000 K are shown in Fig. 3 in comparison with the recent experimental data.[32] There is a very good agreement between these data sets. The sudden change of the MD calculated yttria volume is a manifestation of the thermal instability which occurs at a temperature of about 3125 K. Note that this is not melting. We could calculate the melting temperature quite precisely (precisely with respect to the interatomic interaction model) using, for example, the two-phase method.[4] However, we do not need to know the melting temperature exactly but can give an estimate, using a rough method based on our previous MD simulations for the melting transition. Thus, from simulations of alumina we can say that normally the melting temperature is below the temperature of the thermal instability by somewhat more than 10%.[3] This gives us a melting temperature of yttria between 2700 K and 2800 K, which is very close to the experimental melting temperature.[7,8] The volume change at melting is large, similar to that observed for melting of alumina.[3,4]

Overall, the model [Eq. (1) and Table I] performs reasonably well and our results from MD simulations are close to the results of other (*ab initio* and experimental) methods at moderate pressures and up to high temperatures. This suggests that the model might be applied to calculate structures

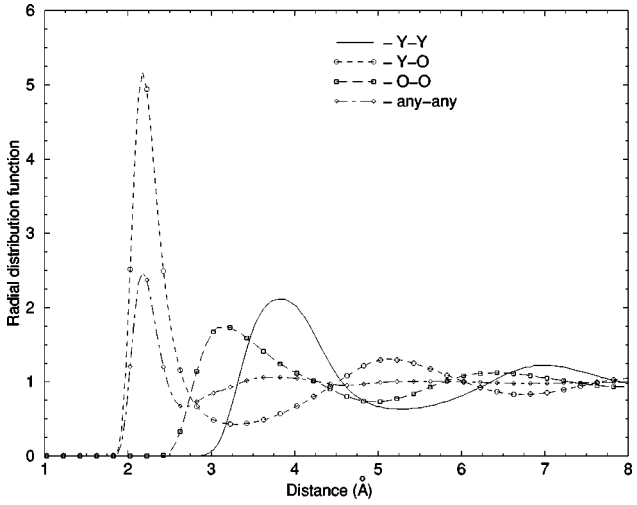

FIG. 4. Radial distribution functions (RDF) calculated at the temperature of 2833 K. The general RDF is indicated as ''any-any'' in the legend.

of liquid and amorphous yttria and gives us a solid ground for an interpretation of the experimental results.

C. Comparison between calculated and experimental structures

To study the structure of noncrystalline yttria we performed MD run at P=1 bar and T=4000 K for 40 000 time steps. The final configuration was saved and served as an initial configuration for runs at a number of temperatures. All these runs consisted of 20 000 time steps to equilibrate the system and then another 20 000 time steps were used to calculate average properties. We also calculated averages each 5000 time steps at the productive stage of each simulation run. No systematic drift was observed by using these intermediate averages. To make sure that the results are not influenced by the duration of the runs we performed several runs of extreme length, up to 200 000 steps. Therefore, the presented results are checked against adjustable parameters variation as explained above in Sec. III A and also against run duration which might be critical when calculating amorphous structure.

The four calculated RDF are presented in Fig. 4 (for details of calculation of RDF see, e.g., the paper by Gutierrez *et al.*[5]). The RDF is rather typical for all liquid and undercooled liquid structures. The general RDF (marked as ''any-any'' in the legend of Fig. 4) shows a strong first peak, a visible second peak and a rather featureless tail in agreement with the experimental data.[7,8] We want to emphasize that the absence of strong peaks in the general RDF at distances larger than the position for the second peak is typical for noncrystalline yttria. Such peaks have not been observed neither in the liquid nor in the amorphous MD simulated yttria at any, as low as 300 K, temperature. Also, there is a very small overlap between the first Y-O and O-O RDF peaks. Therefore, the O-O RDF does not add much intensity to the first peak of the general RDF. The positions of the first (2.25 Å) and the second (3.65 Å) peaks are the same as derived from experimental data.[7,8]

To compare the results of our MD simulations with experimental data,[7,8] we carried out four MD runs at the experimental conditions,[7,8] i.e., at the pressure 1 bar and at four temperatures. RDF's, similar to those shown in Fig. 4, were calculated as well as the density. This was sufficient information to calculate the x-ray scattering static structure factor to compare with the experimental ones.[7,8] This comparison is more appropiate than to compare the pair distribution function, which is derived from the experimental diffraction pattern subject to several assumptions. Partial static structure factors are calculated from the Fourier transform of corresponding partial pair distribution functions by means of

$$S_{\alpha\beta}(q)=\delta_{\alpha\beta}+4\pi\rho(c_\alpha c_\beta)^{1/2}\int_0^\infty [g_{\alpha\beta}(r)-1]\frac{\sin(qr)}{qr}r^2dr, \tag{2}$$

where $c_{\alpha(\beta)}=N_{\alpha(\beta)}/N$ is the concentration of $\alpha(\beta)$ species, ρ is the density, and $g_{\alpha\beta}$ is the radial distribution function of atom β around the α atom.

The x-ray scattering static structure factor can be obtained from the partial static structure factors by weighting them with the x-ray form factors:

$$S_X(q)=\frac{\sum_{\alpha\beta} f_\alpha(q)f_\beta(q)(c_\alpha c_\beta)^{1/2}[S_{\alpha\beta}(q)]}{\sum_\alpha f_\alpha^2(q)c_\alpha}, \tag{3}$$

where $f_\alpha(q)$ are the q-dependent x-ray form factors. The form factors for Y and O are taken from the literature.[33,34]

In Fig. 5 we display the calculated and experimental $S_X(q)$ for four different temperatures. Two of these temperatures (2526 and 2650 K) are below the melting temperature and two of them are above melting (2833 and 3039 K). The agreement is best for the lowest temperature. Even though the agreement becomes worse with increasing temperature, the basic features, namely two distinct peaks, a sharp first peak, a flat second peak and a featureless tail, are all well reproduced and are common for the calculated and experimental[7,8] curves. Note that the scatter of the experimental data becomes larger with increasing temperature. Also, the height of the first peak in the experimental data changes irregularly with temperature with the highest peak at the temperature of 2650 K. While the experimental data shows a strong change of $S_X(q)$ with temperature, the calculated $S_X(q)$ (Fig. 6) depends much less on temperature. This is an indication that no major structural changes occur within a comparatively narrow temperature interval, which is, in our opinion, natural to expect for a noncrystalline structure unless a liquid-liquid transition occurs.

IV. DISCUSSION

There are three things which need to be discussed: first, a comparison with previous MD calculations for the noncrystalline yttria structure;[9] second, a comparison with the structure of amorphous yttria as derived from the experimental

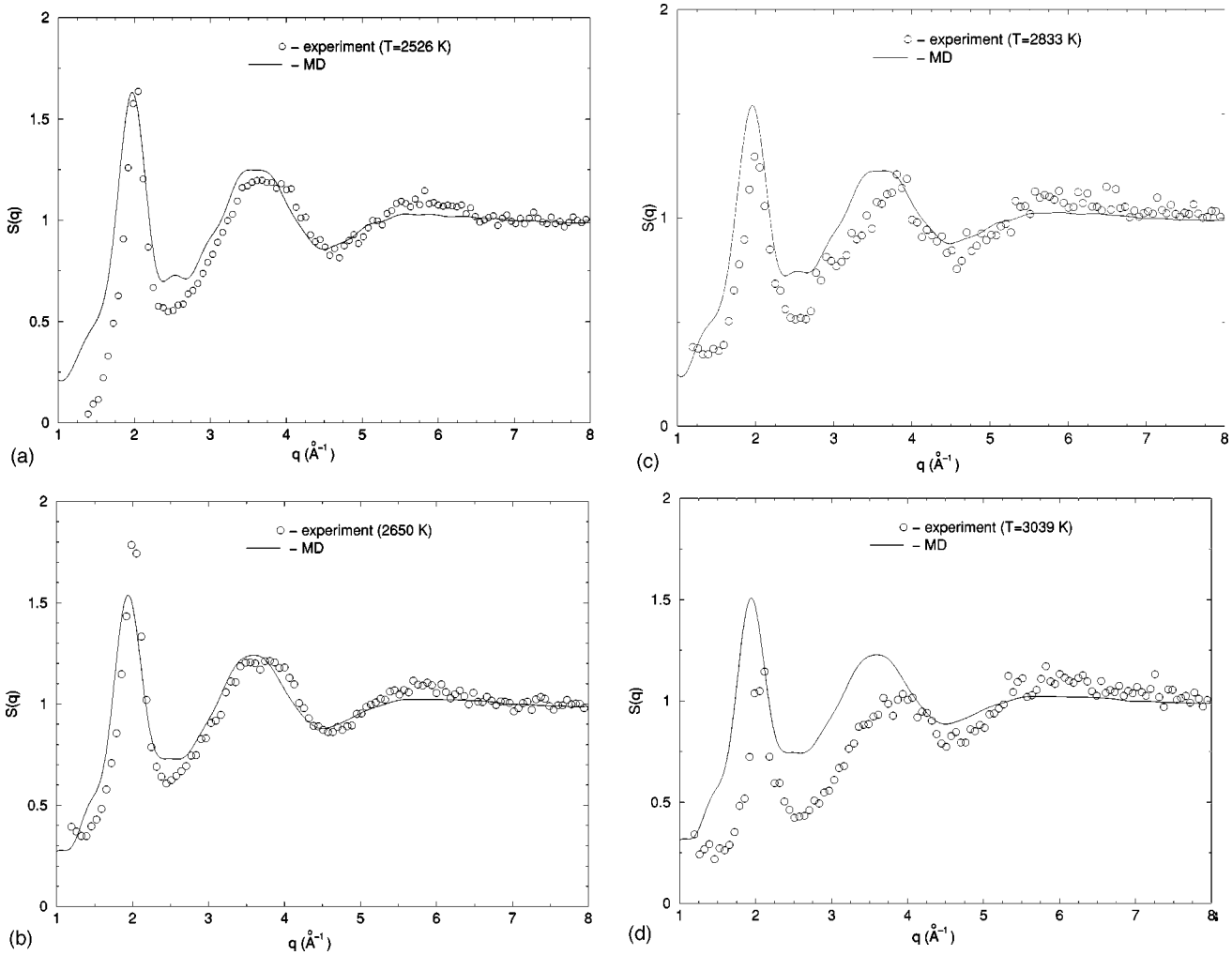

FIG. 5. Structure factor of liquid Y_2O_3 at the pressure of 1 bar, calculated as described in the text and compared with experimental data (Ref. 7) at four temperatures: (a) 2526 K, (b) 2650 K, (c) 2833 K, and (d) 3039 K.

data;[7,8] and, third, the possibility of an alternative, ''light'' amorphous phase.

The authors of a recent paper[9] concerning yttria could not obtain a qualitative agreement between the simulated and experimental structure for noncrystalline yttria, unless they assumed nonstoichiometry in their simulation, namely, a substantial oxygen atom deficit. Though the paper lacks details, it is still possible to make certain remarks concerning the reasons for the mismatch between their simulations and experiment. The general RDF in their paper for stoichiometric yttria exhibits a number of distinct peaks even for large distances. This is typical for a solid structure. This indicates that these simulations gave results which are valid for a solid structure, and, therefore, could not be expected to look like the experimental RDF for amorphous or liquid yttria. However, the authors[9] assumed that yttria under the experimental conditions with a low oxygen fugacity might experience a deficit of oxygen. Therefore they took away a certain amount of oxygen and carried out other runs with nonstoichiometric yttria as a starting configuration. Finally, when a sufficiently

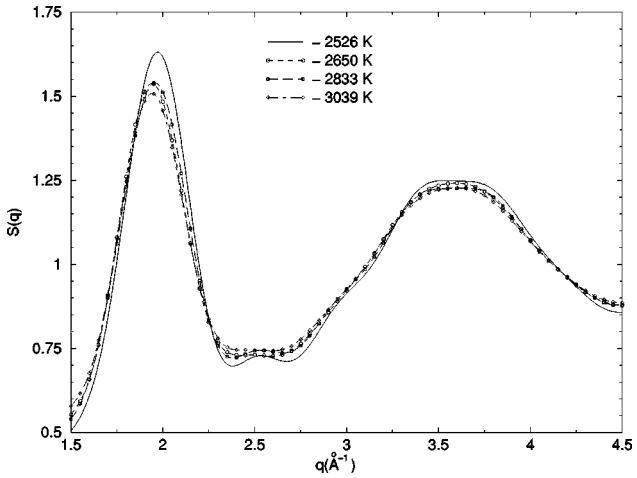

FIG. 6. Structure factor of liquid Y_2O_3 at the pressure of 1 bar calculated at four temperatures indicated in the legend. There is rather subtle change in structure over the considered temperature interval.

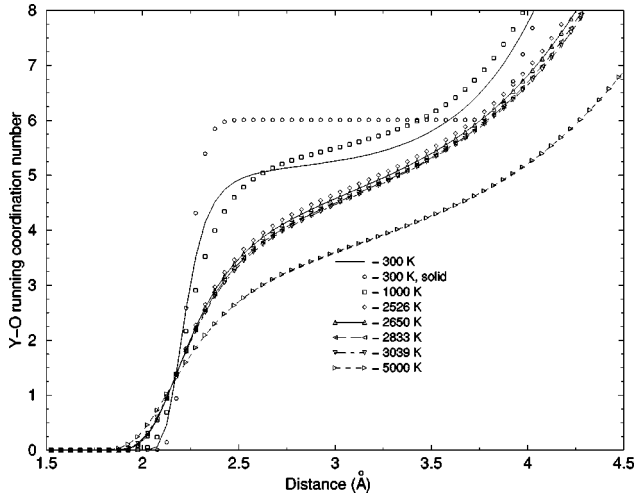

FIG. 7. Y-O running coordination number (RCN, average number of O atoms around Y atom as a function of distance from Y atom) in amorphous and liquid yttria as a function of temperature. RCN in solid yttria is shown for comparison. The number of oxygens in the first shell and the Y-O bond length correspond to the inflection point on the RCN curve, for example, at the temperature of about 3000 K the Y-O bond length is about 3.3 Å and the Y-O RCN is approximately between 4.5 and 5 O atoms.

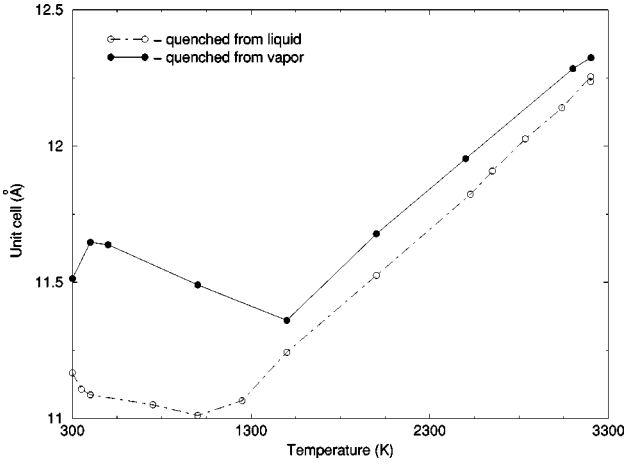

FIG. 8. Volume of yttria, calculated using molecular dynamics method, as a function of temperature at the pressure of 1 bar. Two curves, shown on the figure, are obtained using two different initial configurations of Y and O atoms. The curve, indicated as ''quenched from liquid'' in the legend, was calculated using starting liquidlike configuration of atoms. The curve, indicated as ''quenched from vapor'' in the legend, was calculated using starting gaslike configuration of atoms (see text for details).

large amount of O atoms was taken away the calculated structure qualitatively matched the experimental one. We believe that this happened because the structure with deleted O atoms is less stable than stoichiometric yttria, and, therefore, the match was obtained when yttria in the MD run collapsed. The collapse is the main reason for the match achieved. However, the oxygen deficit is not necessary to achieve a good match with the experimental structure, which is clear from our Fig. 5.

The authors of the experimental paper[7,8] made certain conclusions regarding the structure of noncrystalline yttria based on experimental data. We should note, however, that the primary data is subject to some scatter. Some further technical operations, used to extract the data from RDF also add certain errors. Therefore, these conclusions, even being based on experiment, might be subject to some errors. In particular, the authors conclude that, as the temperature increases, the coordination number (CN) (number of oxygens in the first shell around Y atom) increases, and that the length of the Y-O bond decreases. However, this appears to be a very strange phenomenon, because in order to have CN increasing and the bond length decreasing one has to reach a higher density. Unless the noncrystalline yttria volume decreases with temperature, as contrary to the most usual behavior (temperature expansion is positive for nearly all substances), the obtained judgement of the experimental data appears to be unlikely. In Fig. 7 we illustrate how the Y-O CN changes with distance and with temperature. The CN is 6 in solid yttria and less than 6 in noncrystalline yttria; the CN decreases and the Y-O bond length increases as the temperature increases. We should also note that the first peak of the general RDF, which is responsible for the CN derived from the experiment, is increasingly affected by the O-O RDF when the temperature increases. This might lead to a conclusion of an increase of the Y-O CN with temperature from the experimental data, which do not discriminate between different kinds of atoms. Note (Fig. 7) that in the experimental temperature range the calculated change of the CN and the Y-O bond length are small. However, for a wide temperature range from 300 to 5000 K, the trend becomes quite clear. Somewhat nonmonotonic behavior can be noticed at low temperatures (between 300 and 1000 K) and we shall discuss it next.

The calculated density of amorphous yttria exhibits an irregular dependence on temperature (Fig. 8). Namely, that the volume decreases at temperatures between 300 K and 1000 K and at temperatures above 1000 K it increases again. This can be given a simple physical explanation. The volume behavior means that at low temperatures the atoms have a kinetic energy which does not allow them to explore all the local minima of the energy megabasin. As the temperature increases above 300 K, the atoms are able to visit many more local minima and the volume decreases. On the other hand, the structural thermal expansion acts in the opposite direction. At a temperature above 1000 K the second mechanism apparently dominates and the volume starts to increase. This also explains the irregular behavior of the Y-O RCN in the temperature interval between 300 and 1000 K which is shown in Fig. 7. A similar behavior was also observed in the simulation of amorphous SiO_2.[35]

Another interesting effect which we found is that the amorphous phase of yttria might not be unique and one can talk about several amorphous phases of yttria. The new ''light'' phase of amorphous yttria was obtained by quenching vapor-phase yttria. To do this, the crystalline yttria was first heated above the temperature of evaporization, which is about 6000 K for the given model. The MD simulations, conducted at the temperature of 6000 K and higher, showed that the volume significantly increases compared to the vol-

umes, calculated below approximately 6000 K. To check the nature of this increase, we conducted MD simulations at the temperature of 7000 K for the pressures 1 bar and 10 bars. The volume of yttria at the pressure of 10 bars was approximately 10 times less than the volume at the pressure of 1 bar at the same temperature (7000 K), which clearly suggests, that the simulated configuration is indeed the vapor (or gaslike) phase. The final configuration of Y and O atoms, obtained as a result of the MD run at the pressure of 1 bar and temperature of 7000 K was saved. Then, this configuration was used as an initial configuration when conducting simulations at a number of temperatures as indicated in Fig. 8. Note, that the ''normal'' amorphous phase was obtained exactly in the same way, with the only difference—the initial configuration was saved from the MD run at the temperature 4000 K instead of 7000 K. While at final temperatures above approximately 1500 K the volume of the new ''light'' phase (indicated on Fig. 8 as ''quenched from vapor'') is close to the volume of ''normal'' amorphous yttria (indicated on Fig. 8 as ''quenched from liquid''), the densities are distinctly different at low temperatures. We explain this in the following way. The ''normal'' amorphous phase inherits, in some sense, the structure of liquid yttria. The vapor yttria is substantially much more disordered, with very small first peak in the RDF functions and a nonexistent second peak—this being a typical feature for a vapor phase. When the thermal movement into a local energy minimum position is abruptly hindered, as is the case when quenching to low temperatures, the obtained phase has a higher degree of distortion and, therefore, a larger volume. We carried out extremely long—up to a 0.5 nanosecond—simulations and did not observe any relevant changes compared to the 10 times shorter simulations. The new ''light'' amorphous phase was subject to various perturbations, such as elevated pressure, but demonstrated a considerable stability against these influences. If the ''light'' amorphous phase is brought to a low temperature through the intermediate stage of equilibration at the temperature of 4000 K (where the configuration for the MD simulations of ''normal'' amorphous phase was obtained; see above in Sec. III), we do not obtain a ''light'' phase. This is because diffusion in the liquid phase is significant and the gaslike phase equilibrates into a liquidlike phase. If the quenching would be performed very slow, in contrast with our instant quenching, we would probably obtain the results, different from that shown in Fig. 8 for low temperatures, where the diffusion is low. It is well known[35] that properties of nonequilibrium phases depend on a history of their preparation. In this paper, we point out the principle possibility of obtaining a ''light'' amorphous yttria phase.

V. CONCLUSIONS

Our chosen method to describe the interatomic interactions in yttria is shown to perform sufficiently well to allow for a description of various properties of yttria phases in reasonable agreement with experiment. Based upon our present results, we are led to conclude that the assumption about nonstoichiometric yttria melting[9] is not necessary to get an agreement with experimental data[7,8] on structure of liquid yttria. The temperature dependence of the structure of noncrystalline yttria might be complex and further considerations of its nonunique character should be made.

ACKNOWLEDGMENTS

We are thankful to K. Refson for the MOLDY software package. Discussions with S. Krishnan are gratefully acknowledged. The calculations were performed using Cray T3E at the Swedish National Supercomputer Center in Linkoping. We also wish to thank the Swedish Natural Science Research Council (NFR) and the Swedish Material Consortium 9 for financial support. G.G. was partially supported by FONDECYT (Chile) under Grant No. 1010126.

[1] B. Cockayne and B. Lent, J. Cryst. Growth **46**, 371 (1979).
[2] S. Aasland and P.F. McMillan, Nature (London) **369**, 633 (1994).
[3] A.B. Belonoshko, Phys. Chem. Miner. **25**, 138 (1998).
[4] R. Ahuja, A.B. Belonoshko, and B. Johansson, Phys. Rev. E **57**, 1673 (1998).
[5] G. Gutierrez, A.B. Belonoshko, R. Ahuja, and B. Johansson, Phys. Rev. B **61**, 2723 (2000).
[6] A.B. Belonoshko, R. Ahuja, and B. Johansson, Phys. Rev. B **61**, 3131 (2000).
[7] S. Krishnan, S. Ansell, and D.L. Price, J. Am. Ceram. Soc. **81**, 1967 (1998).
[8] S. Krishnan and D.L. Price, J. Phys.: Condens. Matter **12**, R145 (2000).
[9] L.J. Alvarez, M.A.S. Miguel, and J.A. Odriozola, Phys. Rev. B **59**, 11303 (1999).
[10] R.A. Buckingham, Proc. R. Soc. London, Ser. A **168**, 234 (1938).
[11] A.B. Belonoshko, Geochim. Cosmochim. Acta **58**, 4039 (1994).
[12] A.B. Belonoshko and L.S. Dubrovinsky, Am. Mineral. **81**, 303 (1996).
[13] M. Matsui, Phys. Chem. Miner. **23**, 345 (1996).
[14] M.M. Kuklja, J. Phys.: Condens. Matter **12**, 2953 (2000).
[15] G.J. Kramer, N.P. Farragher, and B.W.H. van Beest, Phys. Rev. B **43**, 5068 (1991).
[16] A. J. Dekker, *Solid State Physics* (Macmillan and Company Limited, London, 1965), pp. 117–128.
[17] J.D. Gale, J. Chem. Soc., Faraday Trans. **93**, 629 (1997).
[18] L. Pauling and M.D. Sappel, Z. Kristallogr. **75**, 128 (1930).
[19] M.G. Paton and E.N. Maslen, Acta Crystallogr. **19**, 317 (1965).
[20] A. Fert, Bull. Soc. Fr. Mineral. Cristallogr. **LXXXIX**, 194 (1966).
[21] B.H. O'Connor and T.M. Valentine, Acta Crystallogr., Sect. B: Struct. Crystallogr. Cryst. Chem. **B25**, 2140 (1969).
[22] J. M. Wills (unpublished); J.M. Wills and B.R. Cooper, Phys. Rev. B **36**, 3809 (1987); D.L. Price and B.R. Cooper, *ibid.* **39**, 4945 (1989).
[23] L. Hedin and B.I. Lundqvist, J. Phys. C **4**, 2064 (1971).
[24] O.K. Andersen, Phys. Rev. B **12**, 3060 (1975).
[25] H. L. Skriver, *The LMTO Method* (Springer, Berlin, 1984).

[26] D.J. Chadi and M.L. Cohen, Phys. Rev. B **8**, 5747 (1973); S. Froyen, Phys. Rev. B **39**, 3168 (1989).
[27] C. Proust, Y. Vaills, Y. Luspin, and E. Husson, Solid State Commun. **93**, 729 (1995).
[28] M. P. Allen and D. J. Tildesley, *Computer Simulation of Liquids* (Clarendon, Oxford, 1987).
[29] K. Refson, MOLDY, Release 2.13, 1998, a general-purpose molecular dynamics code. Available free at http://www.earth.ox.ac.uk/ keith/moldy.html.
[30] W.G. Hoover, Phys. Rev. A **31**, 1695 (1985).
[31] D. Fincham, Mol. Simul. **8**, 165 (1992).
[32] V. Swamy, N.A. Dubrovinskaya, and L.S. Dubrovinsky, J. Mater. Res. **14**, 456 (1999).
[33] D. T. Cromer and J. T. Weber, in *International Tables for X-Ray Crystallography*, edited by J. A. Ibers and W. C. Hamilton (Kynoch Press, Birmingham, 1974), Vol. IV, Chap. 2.2, p. 71.
[34] M. Hemmati, M. Wilson, and P.A. Madden, J. Phys. Chem. B **103**, 4023 (1999).
[35] K. Vollmayr, W. Kob, and K. Binder, Phys. Rev. B **54**, 15 808 (1996).